2003

A 64-pixel Positron-Sensitive Surgical Probe

F. Liu
University of Pennsylvania

J R. Saffer
University of Pennsylvania

Godwin M. Mayers
University of Pennsylvania

Walter Kononenko
University of Pennsylvania, WK@HEP.UPENN.EDU

F Mitchell Newcomer
University of Pennsylvania, mitch@hep.upenn.edu

See next page for additional authors

A 64-pixel Positron-Sensitive Surgical Probe

Abstract

We report on the continued development of a 64-pixel positron-sensitive surgical probe with a dual-layer detector and multi-anode PMT. An 8 x 8 array of this plastic scintillators in teh first layer detects positrons and a matched GSO crystal array in the second layer detects annihilation 511 keV gammas, which are required to be in coincidence with the detected positrons. Also, the 64 PMT anode signals are differentiated and an overshoot threshold is applied to separate the fast decay plastic anode signals from the slower GSO signals. Finally, an energy threshold is applied to the summed anode signal to distinguish 511 keV gammas from the 140 keV gammas commonly used in sentinel lymph node (SLN) surgery. Previously we reported on how these signal selection criteria were individually tested and optimized based on 9 channels of prototype electronics [1-2]. Currently the electronics shave been upgraded to Xilinx® programmable components, allowing on-the-fly alteration of signal selection criteria, and all 64 channels are operational. Initial measurements of the complete 64-pixel probe were conducted using ^{18}F-FDG positron sources and ^{18}F-FDG and ^{99m}Tcphantoms (background 511 keV and 140 keV gammas), simulating lesions in the SLN surgery environment. The average positron sensitivity is measured to be 3.0-7.0 kcps/μCi at different signal selection criteria. The lower bound on sensitivity corresponds to settings optimized for high image resolution and high background rejection ability. The upper bound on sensitivity corresponds to settings optimized for high sensitivity at the cost of lower image resolution and lower background rejection ability. The measured true-to-background contrast in the presence of clinically observed levels of 511 keV and 140 keV background gammas is ~3:1 for a tumor-to-background uptake ratio of 5:1. Performance measurements of the complete 64-pixel probe including sensitivity, true-to-background ratio, and the pixel separation ability are presented.

Disciplines

Physical Sciences and Mathematics | Physics

Comments

Suggested Citation:
Liu, F.; Saffer, J.R.; Mayers, G.M.; Kononenko, W.; Newcomer, F.M.; Karp, J.S.; Lockyer, N.S.; , "A 64-pixel positron-sensitive surgical probe," *Nuclear Science Symposium Conference Record, 2002.* IEEE , Vol.2. pp. 1158- 1162 vol.2, 10-16 Nov. 2002. doi: 10.1109/NSSMIC.2002.1239527

Author(s)

F. Liu, J R. Saffer, Godwin M. Mayers, Walter Kononenko, F Mitchell Newcomer, Joel S. Karp, and N S. Lockyer

A 64-pixel Positron-Sensitive Surgical Probe

F. Liu[1,2], *Student Member IEEE*, J.R. Saffer[2], *Member IEEE*, G.M. Mayers[1], W. Kononenko[1], F.M. Newcomer[1], *Member IEEE*, J.S. Karp[2], *Senior Member IEEE*, N.S. Lockyer[1], *Member IEEE*
Departments of [1]Physics and [2]Radiology, University of Pennsylvania, Philadelphia, PA 19104

***Abstract*-- We report on the continued development of a 64-pixel positron-sensitive surgical probe with a dual-layer detector and a multi-anode PMT. An 8 x 8 array of thin plastic scintillators in the first layer detects positrons and a matched GSO crystal array in the second layer detects annihilation 511 keV gammas, which are required to be in coincidence with the detected positrons. Also, the 64 PMT anode signals are differentiated and an overshoot threshold is applied to separate the fast decay plastic anode signals from the slower GSO anode signals. Finally, an energy threshold is applied to the summed anode signal to distinguish 511 keV gammas from the 140 keV gammas commonly used in sentinel lymph node (SLN) surgery. Previously we reported on how these signal selection criteria were individually tested and optimized based on 9 channels of prototype electronics [1-2]. Currently the electronics have been upgraded to Xilinx® programmable components, allowing on-the-fly alteration of signal selection criteria, and all 64 channels are operational. Initial measurements of the complete 64-pixel probe were conducted using ^{18}F-FDG positron sources and ^{18}F-FDG and ^{99m}Tc phantoms (background 511 keV and 140 keV gammas), simulating lesions in the SLN surgery environment. The average positron sensitivity is measured to be 3.0-7.0 kcps/μCi at different signal selection criteria. The lower bound on sensitivity corresponds to settings optimized for high image resolution and high background rejection ability. The upper bound on sensitivity corresponds to settings optimized for high sensitivity at the cost of lower image resolution and lower background rejection ability. The measured true-to-background contrast in the presence of clinically observed levels of 511 keV and 140 keV background gammas is ~3:1 for a tumor-to-background uptake ratio of 5:1. Performance measurements of the complete 64-pixel probe including sensitivity, true-to-background ratio, and the pixel separation ability are presented.**

I. INTRODUCTION

Small surgical probes have higher sensitivity and resolution than conventional gamma cameras due to their small geometry and reduced distance from the survey area. Such a probe has potential application to tumor bed surveys, melanoma and SLN surgery. These applications have great potential in assisting the staging of cancer treatment and in planning a patient's therapy.

There are several types of beta-sensitive devices under development by other groups [3-9]. Compared to 511 keV gammas from ^{18}F-FDG, the short interaction length of positrons in tissue gives a measurement representative of just the region immediately in front of the probe (~1 – 2 mm). Taking advantage of the high tumor-to-background uptake ratio of ^{18}F-FDG (~10-20), we have built a 64-pixel dual-layer positron-sensitive surgical probe to identify in real time the location of SLNs that have high ^{18}F-FDG uptake, which may indicate metastases. This probe will be able to distinguish positrons from the background gammas, which in the SLN surgery situation consist of both 511 keV gammas from positron annihilation in the body and 140 keV gammas from ^{99m}Tc used to identify the SLNs [10-11].

The detailed design of this positron-sensitive surgical probe with the suppression of background gammas was previously reported [1]. Preliminary performance results including positron sensitivity, pixel separation ability and the true/false ratio based on the 9-channel prototype probe (9-pixel) also were reported [2]. In this paper the performance results from all 64 channels of newly optimized and miniaturized electronics are presented, including lesion contrast measurements in the presence of gamma background, sensitivity, and pixel separation ability.

II. PROBE DESIGN

Our positron-sensitive surgical probe consists of a multi-anode PMT (Hamamatsu model H7546) and an 8x8 element two-layer detector array of plastic scintillators (BC404, Bicron) and GSO crystals (Hitachi). Fig. 1 illustrates the main probe components: a matched array of thin plastic scintillators (2 mm x 2 mm x 0.5 mm) optically coupled to 2 mm x 2 mm x 10 mm GSO crystals. Each array element is optically isolated using $CaCO_3$ reflectors. The GSO crystals are optically coupled to the multi-anode PMT; which has an 8 x 8 array of anodes. Each anode is 2 mm x 2 mm, spaced 2.3 mm apart.

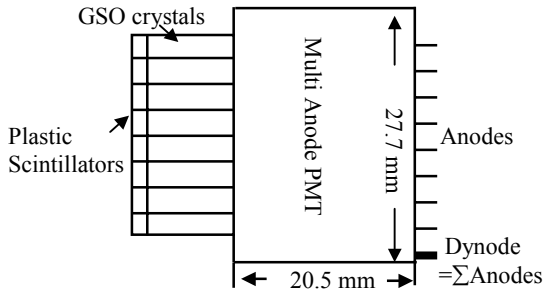

Fig. 1. Schematic design of the dual-layer positron-sensitive surgical probe. The BC404 plastic scintillators are 2 mm x 2 mm x 0.5 mm, while the GSO crystals are 2 mm x 2 mm x 10 mm. Each array element is optically isolated using $CaCO_3$ reflectors. The GSO crystals are optically coupled to the multi-anode PMT; which has an 8 x 8 array of anodes. The anodes of the PSPMT are 2 mm x 2 mm, spaced 2.3 mm apart.

0-7803-7636-6/03/$17.00 ©2003 IEEE.

Our probe uses three selection criteria to identify positrons and suppress background gammas from annihilation 511 keV gammas elsewhere in the body and

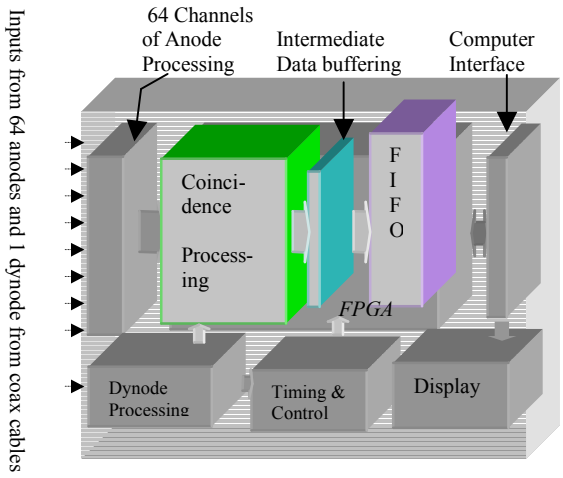

Fig. 2. Schematic design of the electronics of the final 64-channel probe assembly, which will be connected to the detector array by coax cables.

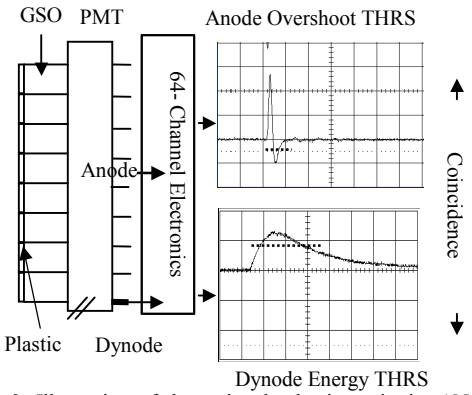

Fig. 3. Illustration of three signal selection criteria: AN OS THRS, DY energy THRS and the coincidence between the AN OS and the DY energy.

140 keV gammas due to ^{99m}Tc. The schematic for the electronics of the complete 64-pixel probe assembly is shown in Fig. 2. In the 64 anode processing module, a differentiation technique is applied to the anode signals to produce an overshoot for fast plastic signals compared to slower GSO signals. An energy threshold on this overshoot (AN OS THRS) reduces false positron signals in the plastic due to background gammas. In the dynode-processing module, the dynode signal is integrated and an energy threshold on this integrated dynode signal (DY energy THRS) differentiates 511 keV gammas from other background gammas. In the coincidence-processing module, a timing window requires coincidence between the annihilation 511 keV gammas and the detected positrons. These three signal selection criteria are shown in Fig. 3. The count vs. probe pixel information (count intensity of each pixel) is shown in the display module. These three selection criteria were individually tested and optimized, based on the 9 channels of prototype electronics. The performance measurements of that system showed the probe had a range of sensitivity to positrons (2.0–6.0 kcps/μCi) at different signal selection criteria. By choosing a high sensitivity we have lower background rejection ability and a lower image resolution; by choosing a lower sensitivity we will gain high background rejection ability and a high image resolution [2].

Now the electronics have been further optimized and miniaturized, especially the shaping circuits for the dynode signal and the 64 anode signals, and the timing logic processing circuit. We have developed a 64-pixel probe assembly based on this newly optimized and miniaturized 64-channel electronics.

III. METHODS

To measure the performance of the probe, we used the following method to simulate a lesion and the gamma background. Based on spherical geometry and the attenuation coefficient for positrons in tissue (μ=25.12 cm^{-1}) we calculated the positron flux on a single 2mm x 2mm detector element in contact with a 1-cm diameter tumor to be 0.3% of the total tumor activity flux. This positron flux was then modeled by pieces of papers soaked in ^{18}F-FDG of known concentration. The sources were air-dried, assayed then placed directly on the detector array. To simulate the 511 keV gamma background in a patient's normal tissue, a cylindrical bottle (d=8 cm >> 1-cm diameter of simulated lesion) was filled with 500 cc of ^{18}F-FDG. To simulate the 140 keV gamma background present in the SLN surgery environment, a smaller cylindrical bottle (d=5cm) was filled with ^{99m}Tc at a concentration sixty times higher than the 511 keV gamma background, in order to simulate the local injection of 1 mCi ^{99m}Tc used in SLN surgery. The base of the bottles rested atop the detector array, with the paper positron source sandwiched in between.

IV. RESULTS

We optimized the 64-channel probe performance, including background rejection ability, positron sensitivity and image resolution, by adjusting the AN OS THRS and the DY energy THRS. A higher AN OS THRS and DY energy THRS rejects background gammas more efficiently, thus giving a better true-to-background contrast, also giving better image resolution, but at the cost of reducing the sensitivity. Optimum performance was achieved using: AN OS THRS=130 keV, DY energy THRS=200 keV. Unless otherwise noted, the following results were obtained using these optimized signal selection criteria.

A. Lesion Contrast

To test the performance of the 64-channel probe, we measured lesion contrast. Two positron sources of 2 mm x 2 mm and 4 mm x 4 mm were made containing 0.01 μCi and 0.028 μCi of ^{18}F-FDG respectively, equivalent to the positron flux incident on the detector from 1-cm diameter

lesions with 3.2 μCi/cc of activity and 2.2 μCi/cc, respectively. The sources were positioned as shown in Fig. 4 (a). To simulate a patient's normal tissue activity, the ^{18}F-FDG phantom was filled with a concentration of 0.43 μCi/cc ^{18}F-FDG, equivalent to a tumor-to-background uptake ratio of ~8:1 for the 2 mm x 2 mm source and ~5:1 for the 4 mm x 4 mm source. First we recorded the count rates in each pixel for the positron sources alone. Then we recorded the count rates in the presence of the ^{18}F-FDG phantom. The count intensities of the 64 pixels without/with ^{18}F-FDG background are shown in Figs. 4(b)-(c). Note that each line in Figs. 4(b)-(c) corresponds to the center of each pixel. The comparison between Fig. 4(b) and Fig. 4(c) shows that at the optimized signal selection criteria (AN OS THRS=130 keV, DY energy THRS=200 keV) the two paper sources can be identified clearly even in the presence of the ^{18}F-FDG background. At a tumor-to-background uptake ratio of 5:1, the lesion contrast is ~3:1, as seen in Fig. 4(c).

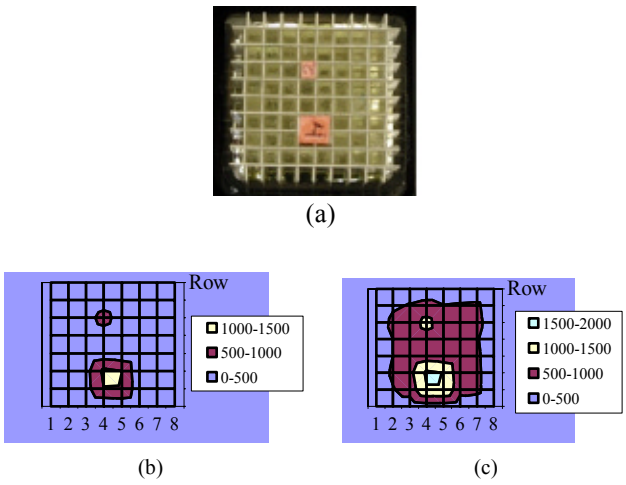

Fig. 4. The identification of 2 simulated lesions: 2 mm x 2 mm and 4 mm x 4 mm positron sources (a) Top view of the position of the two positron sources on the 64-pixel probe (b) 2-D surface plot of counts per minute without 511 keV gamma background (c) 2-D surface plot of counts per minute with 511 keV gamma background. Lesion contrast is ~8:1 for smaller source, and ~5:1 for larger source. Note that grid lines go through the centers of the detectors.

For a realistic test of the 140 keV gamma rejection power of the probe, the same ^{18}F-FDG positron sources were measured in the presence of a ^{99m}Tc phantom filled with a ^{99m}Tc concentration of ~21 μCi/cc, which is ~60 times higher than the background ^{18}F-FDG concentration used in the previous experiment. This higher background level simulates the SLN surgery procedure of locally injecting ^{99m}Tc around the primary tumor. Using a similar sequence of measurements as the previous experiment, we measured the count rate in each pixel in the presence of

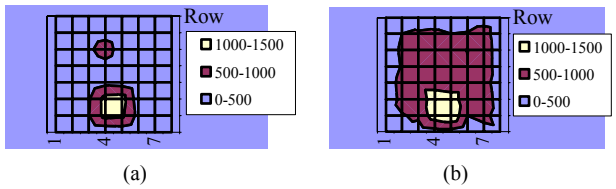

Fig. 5. 2-D surface plot of count per minute showing the lesion identification capability with background ^{99m}Tc: (a) At AN OS THRS=130 keV, DY energy THRS=200 keV (b) At AN OS THRS=130 keV, DY energy THRS=0 keV

the ^{99m}Tc phantom. The two simulated lesions were both identified clearly at the optimized probe thresholds (AN OS THRS= 130 keV, DY energy THRS =200 keV), as seen in Fig. 5(a). Fig. 5(b) shows the importance of placing an energy threshold on the dynode signal. Without that threshold (DY energy THRS=0 keV), so many background 140 keV events are accepted that the 2 mm x 2 mm positron source cannot be distinguished.

B. Positron Sensitivity

Our probe uses an 8 x 8 array of 2 mm x 2 mm detector pixels. In order to investigate the sensitivity of the probe, count rates from a 5 mm x 5 mm positron source of ^{18}F-FDG (0.777 μCi) were measured. The ^{18}F-FDG source was placed directly on the front surface of the plastic scintillator. Due to the limited geometry size of the 8 x 8 pixel array, the detection efficiency of the annihilation 511 keV gammas of the edge GSO crystal pixels is lower than that of the center pixels. To measure the magnitude of this effect on the probe's sensitivity, a positron source was tested at three different locations: at the center, the left top, and the right bottom of the detector face.

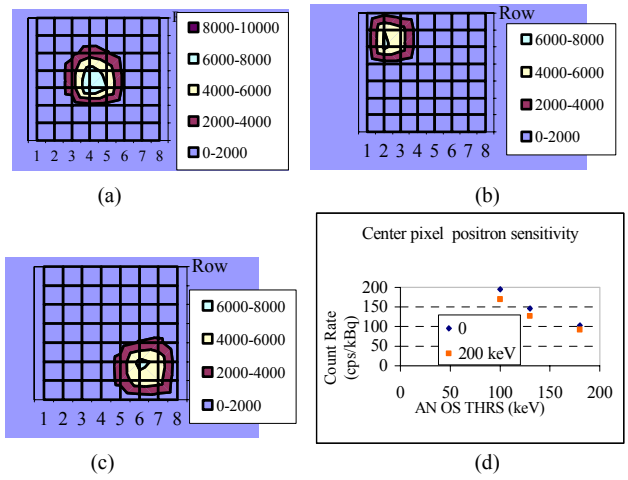

Fig. 6. Count rate measurements of a 5mm x 5 mm positron source (from ^{18}F-FDG) at three different locations on the probe: (a) On the center pixels (b) On the bottom right corner, and (c) On the left top corner. (d) Calculated sensitivity of the center pixels at different AN OS THRS (100 – 180 keV) and DY energy THRS (0 - 200 keV).

Figs. 6 (a)-(c) shows the measurements from the same source at the three different locations. The counts shown in these three figures were all accumulated for 10 seconds and all decay-corrected to the same time. The center of the detector array has the highest sensitivity (3.4-7.2 kcps/μCi); while the left top corner and the right bottom corner have a 15% lower sensitivity (2.9-6.3 kcps/μCi). The sensitivity of the center pixels at different signal selection criteria is shown in Fig. 6(d), illustrating how sensitivity falls off as the DY energy THRS and anode OS THRS are raised, due to the exclusion of lower-energy positrons from the deeper layers of the tissue.

C. Pixel Separation

Pixel separation ability is an important performance parameter for an imaging surgical probe. It determines how well two nearby hot spots can be distinguished. Experiments were conducted using two different hot spot arrangements shown in Figs. 7(a) and 7(d). The hot spots were created by filling 1 mm diameter, 1 mm deep holes in a lucite block with ^{18}F-FDG. First a four point source structure of ^{18}F-FDG (shown in Fig. 7(a)) was placed on the 8 x 8 detector array and the count rates from each of the 64 pixels were recorded. The corresponding 2-D surface plots for measurements taken at two AN OS THRS are shown in Figs. 7(b)-(c). The comparison between Fig. 7(b) and Fig. 7(c) shows that a higher AN OS THRS improves the pixel separation by (a) rejecting more of the small signals generated from the small amount of the shared light in the neighboring pixels, and (b) rejecting background counts more efficiently. At the higher AN OS THRS the spatial resolution approaches the theoretical limit of 2 mm, the size of the detector elements.

In order to quantify the pixel separation ability, a peak-to-valley ratio was calculated by comparing the count rate in the pixel with the point source to the average count rate in its four nearest neighbors. The results are shown in Fig. 7(f). At the optimized parameters, the peak-to-valley ratio is 3.6. At a higher AN OS THRS of 180 keV the peak-to-valley ratio improves to 5.0 but at the expense of a 28% decrease in sensitivity.

Next a diagonal-cross point source structure (shown in Fig. 7(d)) was measured. The 2-D surface plot is shown in Fig. 7(e). Fig. 7(b) and Fig. 7(e) show that the pixel(s) with the point source(s) can be clearly identified at the optimized AN OS THRS (130 keV) and DY energy THRS (200 keV). When choosing the optimum signal selection criteria, however, we need to consider all performance parameters including the sensitivity, background rejection ability and image resolution. Because the probe's electronic components are programmable, the choice of signal selection criteria can be tuned for different imaging situations.

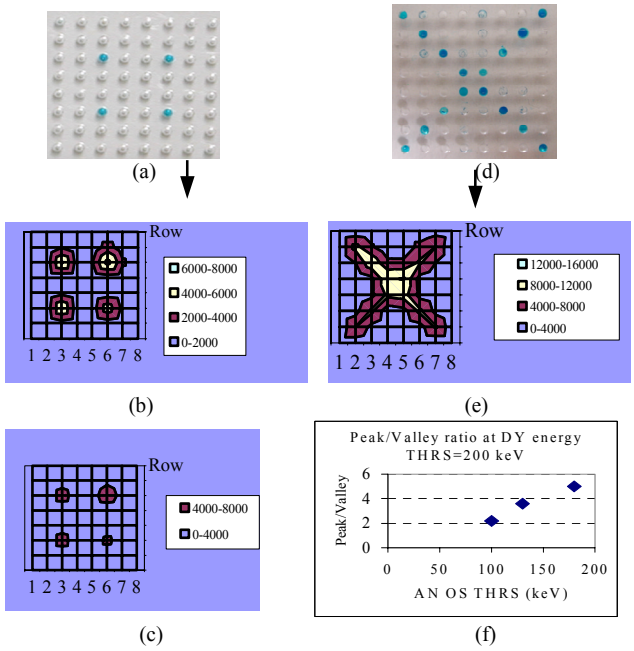

Fig. 7. 2-D image showing the hot spot separation using 2 different point source structures (each point is 1.0 mm deep with 1-mm diameter) (a) A 4 point source structure (b) The corresponding 4 point source structure image at AN OS THRS =130 keV (c) The corresponding 4 point source structure image at AN OS THRS=180 keV (d) A diagonal-cross point source structure (15 point sources) (e) The corresponding diagonal-cross point source structure image at AN OS THRS = 130 keV (f) Peak to valley ratio for the 4 point source structure at DY energy THRS=200 keV and different AN OS THRS (100 - 180 keV)

V. DISCUSSION

A 64-pixel positron-sensitive surgical probe has been built based upon a dual-layer plastic and GSO detector array and a multi-anode PMT. Our probe has an intrinsic spatial resolution of 2 mm with good true-to-background ratio. Detailed study of the sensitivity to positrons and background gammas suggests the AN OS THRS, the DY energy THRS (energy information from the GSO crystal layer) and the coincidence requirement give high rejection power for 140 keV gammas and acceptable rejection ability for 511 keV gammas, which leads to good true to background ratio (3:1 at a tumor-to-background uptake ratio of 5:1). The complete 64-pixel probe has the same true-to-background ratio as the 9-channel prototype probe, but has better positron sensitivity due to the increased detector area. The positron sensitivity ranges from 3 to 7 kcps/μCi at different signal selection criteria. Furthermore, this 64-pixel probe is able to survey a larger area (8 x 8 pixel area of 18.1 x 18. 1 mm^2), and provide spatial discrimination and shape of a lesion.

The first proposed application of this probe is to detect positron events from ^{18}F-FDG in lymph nodes. We have conducted phantom tests simulating the SLN surgery environment, demonstrating a true positron count to background gamma count ratio of ~3:1 for a tumor-to-

background uptake ratio of ~5:1, even in the presence of a high ^{99m}Tc background.

The probe operation is flexible and the signal selection criteria can be tuned for either a higher true/background ratio or a higher sensitivity. Therefore this probe design may have additional applications. For instance it could be used during tumor resection surgery to detect tumor residue or to delineate the edge of a tumor. In addition, the probe might also be operated as a non-imaging gamma probe to guide the surgeon in locating the SLNs, then be switched to positron-sensitive mode to determine whether the SLN has high ^{18}F-FDG uptake, which might indicate metastases.

VI. ACKNOWLEDGMENTS

This work was supported by the U.S. Dept. of Energy grant No. DE-FG02-88ER60642 and a Society of Nuclear Medicine Education and Research Foundation grant.

We thank Rex A. Saffer for his kind help with the tumor model calculation.

VII. REFERENCES

[1] F. Liu, et al., "Design and Performance of a Portable Positron-Sensitive Surgical Probe", IEEE MIC conference record, October 2000.

[2] F. Liu, et al., "Performance of a Dual-Layer Positron-Sensitive Surgical Probe", IEEE MIC conference record, October 2001.

[3] R.R. Raylman, "Performance of a dual, solid-state intraoperative probe system with ^{18}F, ^{99m}Tc, and ^{111}In," J. Nucl. Med., vol. 42(2), pp. 352-360, February 2001.

[4] F. Daghighian, et al., "Intraoperative beta probe: a device for detecting tissue labelled with positron or electron emitting isotopes during surgery," Med. Phys., vol. 21(1), pp.153-157, January 1994.

[5] M.P. Tornai, et al., "A miniature phoswich detector for gamma-ray localization and beta imaging," IEEE Trans. Nucl. Sci., vol. NS-45(3), pp.1166-1173, June 1998.

[6] Commercial beta-sensitive probes are manufactured by IntraMedical Imaging LLC, 1444 Carmelina Ave., Suite 227, Los Angeles, CA 90025 and by Photon Imaging, Inc., 19355 Business Center Dr., Suite 8, Northridge, CA 91324.

[7] E.J. Hoffman, et al., "Intraoperative probes and imaging probes," Eur. J. Nucl. Med., vol. 26(8), pp. 913-935, August 1999.

[8] M.P. Tornai, et al., "Investigation of microcolumnar scintillators on an optical fiber coupled compact imaging system," IEEE. Trans. Nucl. Sci., Vol. 48(3), pp. 637 –644, June 2001.

[9] M.P. Tornai, et al., "A novel silicon array designed for intraoperative charged particle imaging," Medical Physics, vol.29(11), pp.2529-40, November 2002.

[10] Private communications: University of Pennsylvania Medical Center investigators: A. Alavi, M.D. and E.F. Conant, M.D., Dept. of Radiology, B.J. Czerniecki, M.D., Ph.D. and I. Bedrosian, M.D., Dept. of Surgery.

[11] B.J. Czerniecki, et al., "Immunohistochemistry with pancytokeratins improves the sensitivity of sentinel lymph node biopsy in patients with breast carcinoma," Cancer, vol. 85(5), pp. 1098-1103, March 1999.